

Synthesis and Characterization of Magnesium Ferrite Materials

Dr. Sabah Mohammed Ali Ridha

Applied Science Department, University of Technology/Baghdad

Email: sabahyagmur@yahoo.com

Ghead Khalaf Salman

Applied Science Department, University of Technology/Baghdad

Received on: 7/1/2013 & Accepted on: 26/11/2013

ABSTRACT

NiZnMg-Ferrite Nano ceramics were prepared by using sol-gel auto combustion method, these ferrites then pelletized and sintered at different temperatures (1000, 1100 and 1200 °C). Ferrite samples showed spinel structure and inherent properties of high electrical resistivity, low electrical losses and high theoretical densities. Therefore, these ferrites have a potential candidate for high frequency applications. The electrical and structural properties of $Ni_{0.7-y}Zn_{0.3}Mg_yFe_2O_4$ (where; $y= 0, 0.1, 0.2$ and 0.3) were studied and that shows an effect of chemical composition on the electrical, structural, and physical properties depending on Mg content in the Ferrite. Chemical phase analysis carried out by x-ray diffraction spectrum confirms the formation of ferrite Nanopowders with size (22.6 nm), and found that the lattice parameters and particle sizes increase, while theoretical density and porosity decreases with increasing of Mg content in the NiZnMg Ferrites. Resistivity of all samples has been measured at temperatures in the range of (300-540 K), which decreases with increasing of temperatures like a semiconductor behavior.

Keywords: Ferrites, Nano-Magnetic Materials, Sol-Gel Methods, Mg-Ferrites.

تصنيع ودراسة خصائص مواد فيرايتات المغنسيوم

الخلاصة

حضرت فيرايتات (النيكل- زنك-مغنسيوم) النانوي بطريقة سول- جل ذو الاحتراق الذاتي, إذ تم كبسها الى اقراص صلبة وتلييدها عند درجات حرارة مختلفة (1000, 1100, 1200 م⁰). وقد اظهرت النماذج الفيراييتية بامتلاكها التركيب السبنلي ذات خصائص متميزة بكثافة نظرية ومقاومية كهربائية عاليتين علاوة على امتلاكها قيم فقد كهربائي واطئة, لذا فان هذه المواد تستخدم في تطبيقات الاجهزة التي تعمل ضمن الترددات العالية. تمت دراسة الخصائص التركيبية والكهربائية لـ $Ni_{0.7-y}Zn_{0.3}Mg_yFe_2O_4$ ($y=0, 0.1, 0.2, 0.3$) كما ولوحظ تأثير التركيب الكيميائي في الخواص الكهربائية والتركيبية والفيزيائية اعتمادا على محتوى ايونات المغنسيوم في الفرايت. وتم الحصول على مسحوق فيرايت بحجم (22,6 نانومتر) من خلال فحص حيود الاشعة السينية ووجد بان ثابت الشبكة وحجم الدقائق الفيراييتية يتزايدان بينما تتناقص المسامية والكثافة النظرية عند زيادة ايونات المغنسيوم في فرايتات النيكل- مغنسيوم- زنك. وقد تم قياس المقاومة النوعية لكافة النماذج الملبدة عند درجات

حرارة تتراوح بين (300-540 كلفن) ووجدت بأنها تتناقص مع ارتفاع درجة الحرارة يشابه سلوك أشباه الموصلات.

INTRODUCTION

The name "Ferrite" deduces that iron oxide Fe_2O_3 is generally the common oxide to all ferrite. Structural and electric properties of ferrites can be changing by controlling the manner of preparation and type of materials used, amount of material added and sintering temperatures. [1]. Ferrites have an enormous impact over the applications of magnetic materials. The resistivity of ferrites at room temperature can vary from 10^{-2} to 10^{11} Ω -cm, depending on their chemical composition [2]. They are considered superior to other magnetic materials because they have low electric losses and high electrical resistivity. Ferrites have good magnetic properties at the same time are the insulating materials so it is preferred in industries which operate within the high frequency up to 10 MHz, ferrites have high permeability's up to 30,000 and exhibit dielectric properties, exhibiting dielectric properties means that even though electromagnetic waves can pass through ferrites, they do not readily conduct electricity. This also gives them an advantage over iron, nickel and other transition metals that have magnetic properties in many applications because these metals conduct electricity,[3]. Due to rapid progress in the fabrication and processing of nanostructures, ferrite magnetic materials can be made in the range of nanometer (1-100) nm. The chemical and physical properties of nano-materials can significantly differ from those of bulk materials of same chemical composition [4]. And now possible to realize a broad variety of geometries, crystalline textures, and chemistries of nanostructures. The structures can be fabricated using a variety of magnetic materials, with different local magnetic properties and crystalline textures.

Suitable control of properties and response of nanostructures can lead to new devices and technologies. Several research groups are involved in the investigations of spinel oxide nanoparticles because of their potential applications in magnetic devices, microwave technology and high-density magnetic recording media, etc. [58].

MATERIAL AND METHOD

Material

Ferrite powders were prepared by sol-gel auto combustion method. Analytical grade Nickel Nitrate $[Ni(NO_3)_2 \cdot 6H_2O]$ with purity (>99.9%), Magnesium Nitrate $[Mg(NO_3)_2 \cdot 6H_2O]$ with purity (>98%), Zinc Nitrate $[Zn(NO_3)_2 \cdot 6H_2O]$ with purity (>98%), Iron Nitrate $[Fe(NO_3)_3 \cdot 9H_2O]$ (with purity >97%) and Citric acid $[C_6H_8O_7 \cdot H_2O]$ were used as raw materials in auto combustion method. All the chemicals were from fluka AG Company.

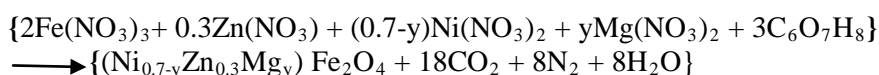
Ferrite synthesis

The sol-gel auto combustion synthesis process was used to prepare substituted Mg ions in Ni-Zn ferrites ($Ni_{0.7-y}Zn_{0.3}Mg_yFe_2O_4$), where $y = 0, 0.1, 0.2, 0.3$.

Table (1) Symbols of the ferrite powder and samples and their compositions.

Ferrite Composition	Symbol of ferrite powders	Sintering at 1373 K
$Ni_{0.7}Zn_{0.3}Fe_2O_4$	D	D2
$Ni_{0.6}Zn_{0.3}Mg_{0.1}Fe_2O_4$	E	E2
$Ni_{0.5}Zn_{0.3}Mg_{0.2}Fe_2O_4$	F	F2
$Ni_{0.4}Zn_{0.3}Mg_{0.3}Fe_2O_4$	G	G2

Ferrite powder was synthesized by an amount of 10 gm per batch. Metal nitrates and Citric Acid are mixed with 80 ml of distilled water as in Figure (1-a). The mixture, placed in a glass beaker, was homogenized by continuous stirring by magnetic hot plat-stirrers model (LMS-1003). The pH of the solution was adjusted to (~7) using ammonia solution and then heated on a hot plate at 60°C half hour and then the temperature is increase to 80°C, as The chemical equation $Ni_{0.7-y}Zn_{0.3}Mg_yFe_2O_4$ is:



With continuous heating it was initially transformed from sol into gel then the gel dried at 120°C about three hours as shown in Figure (1- b) .The dried gel was placed in the oven at 200 °C. Upon ignition, dried gel burnt in a self-propagating combustion manner until all gels were completely burnt out to form a fluffy loose structure as shown in Figure (1-c). The fluffy material was ground to get ferrite powder, Figure (1- d) show that. The as-burnt ash was calcined at 500°C for 3 hrs, to get better crystallization and homogeneous cation distribution in the spinel crystallite, finally was grounded to get ferrite nano powders.



Figure (1) Photograph of (a) nitrate-citrate solution, (b) dry gel, (c) Auto combustion reaction and (d) burnt ash powder.

All composition which refers to ferrites can be prepared in the same way where in each time the amount of Zn, Mg and Ni are changed to produce ferrites with different composition as show the Table (1). Pellet formation, Die is very essential part for making pellets, and commonly made of hard steel. Powders are mixed with 1.5 wt% PVA (Polyvinyl alcohol) as a binder [10]. Here after cold pressed by hydraulic press applied into pellets of 15mm and 12mm diameter under un- axial pressure of ($2 \times 10^3 \text{ Kg/cm}^2$), the product is called green samples. The green samples were sintered at different temperatures in the range of 1000, 1100 and 1200°C. During sintering process, inter diffusion takes place between adjacent particles and they stick together. The porosity is reduced by the diffusion of vacancies to the surface; heat treatment was carried out in step to promote crystallization and to avoid sample damaging. When the sample is ready for testing, silver paste applied on the two faces of the sintered samples (used for electrical measurement only) for improving the electrical conductivity between pellet and the electrodes.

EXPERIMENTAL CHARACTERIZATION

X-ray characteristic measurements

Ferrite Phase formations of calcined ferrite powders and sintered samples were studied by the powder x-ray diffraction performed with a Diffract-meter (DMA-2601). The wave length of x-ray is equals to 0.15406 nm. The crystallite sizes of the samples were determined from x-ray line broadening using the Sherrer's equation [9] as follows;

$$D = 0.9 \lambda / \beta \cos \theta \quad \dots (1)$$

Where, D is the crystallite size, λ is the wavelength of the radiation, θ is the Bragg's angle and β is the full width at half maximum (FWHM). Lattice parameter (**a**) is the parameter defining the unit cell of a crystal lattice. It is also known as lattice constant. Lattice constant refers to the constant distance between the lattice points.[11]. It is calculated using Equation;

$$a = \lambda (h^2 + k^2 + l^2)^{1/2} / 2 \sin \theta \quad \dots (2)$$

Where, (**a**) is lattice parameter, (λ) is the wavelength of the radiation, (θ) is the Bragg's angle and ($h \ k \ l$) is Miller index. The x-ray density (theoretical density) is equal to the weight of atoms in unit cell/ volume of unit cell. Spinel or cubic crystal structure contains 8 formula units in one unit cell, and expressed as following:

$$d_x = 8 M_w / N_a a^3 \quad \dots (3)$$

where, d_x represents x-ray density or theoretical density (gm/cm^3), (N_a) represents Avogadro's number, M_w is the molecular weight and (**a**) is the lattice parameter of unit cell.

DC-electrical resistivity

DC-electrical resistivity of ferrites depends upon the thermal history of the processing in addition to the composition of the ferrites. LCR meter model (889B bench) was used to measure the resistance R (ohm), and find the resistivity by the relation:

$$\rho = R A / L \quad \dots (4)$$

Where (ρ) is the resistivity (ohm. m), R is the resistance. A (in meter square) represents the cross section area of the pole; L (in meter) is the thickness of pellet. The DC-electrical resistivity measurement was carried out at temperatures in rang (300-540 K) using laboratory designed holder.

$$\rho = \rho_0 \exp(\Delta E_a / T K_B) \quad \dots(5)$$

where, ρ is the resistivity, ρ_0 is resistivity at room temperature and E_a is the activation energy required for hopping of an electron from one site to another. Energy of activation for hopping (E_a) is calculated from the slope of the linear plot of ($\ln\rho$) versus $1/T$:

$$\Delta E_a = \text{Slope} * K_B * 1000 \quad \dots (6)$$

RESULTS AND DISCUSSION

Structure properties

Figures (2) and (3) for samples E ($y=0.1$) and G ($y=0.3$) respect, show X-ray diffraction patterns of the ferrite powders $\text{Ni}_{0.7-y}\text{Zn}_{0.3}\text{Mg}_y\text{Fe}_2\text{O}_4$ (where, $y=0.1$ and $y=0.3$) calcined at 773K. From these figures it is clear that samples show good crystallization, with well defined diffraction peaks. This structure can be considered as a single phase spinel structure with no extra peaks correspond to any un-reacted oxides as shown in figures of samples (E) and (G). The planes (220), (311), (400) and (511) in the diffraction pattern confirm the formation of pure phase spinel structure in all samples, while is appeared oxide phase denote by (*) in sample G2 (sintered at 1373 K) as shown in Figure (5), that may be evaporation of Zn ion and then oxidant in the surface of the sample. The decrease in broadening x-rays spectrum decreases with the increase in sintering temperature attributes the grain growth of the crystallites at higher temperatures as shown in Figures (4 and 5) for sintered samples (E2) and (G2).

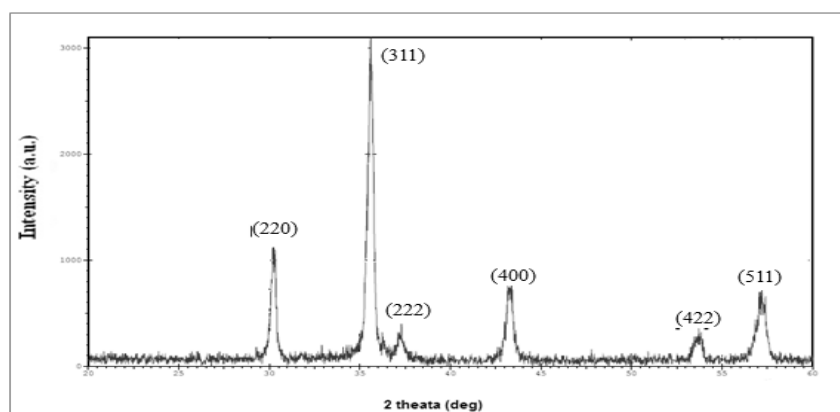


Figure (2) XRD patterns of calcined at 773^ok sample (E)
 $\text{Ni}_{0.6}\text{Zn}_{0.3}\text{Mg}_{0.1}\text{Fe}_2\text{O}_4$.

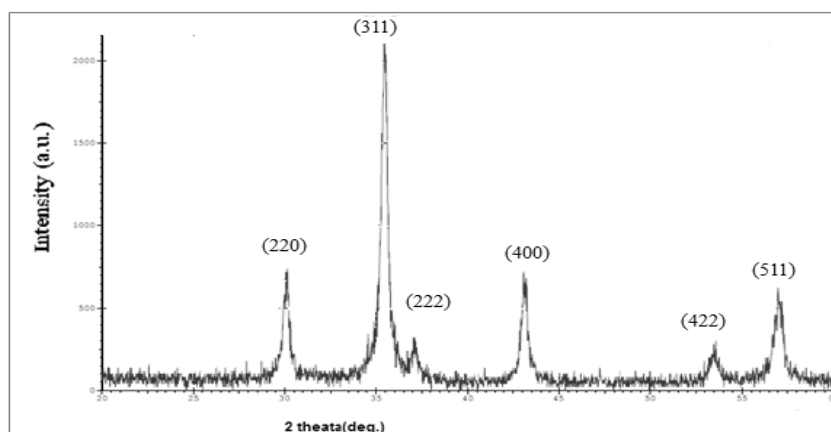


Figure (3) XRD patterns of calcined at 773⁰k sample (G)
 $\text{Ni}_{0.4}\text{Zn}_{0.3}\text{Mg}_{0.3}\text{Fe}_2\text{O}_4$.

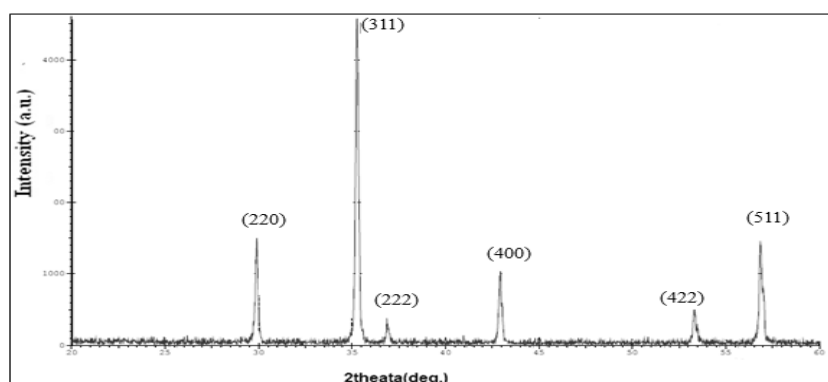


Figure (4) XRD patterns of sintered at 1373⁰k sample (E2)
 $\text{Ni}_{0.6}\text{Zn}_{0.3}\text{Mg}_{0.1}\text{Fe}_2\text{O}_4$.

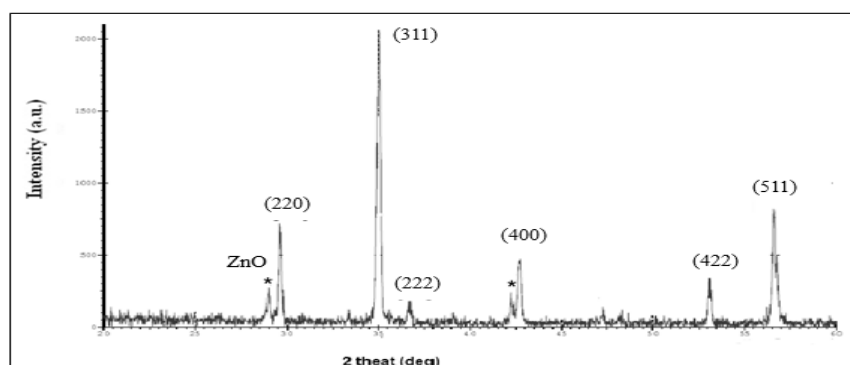


Figure (5) XRD patterns of sintered at 1373⁰k sample
 (G2) $\text{Ni}_{0.4}\text{Zn}_{0.3}\text{Mg}_{0.3}\text{Fe}_2\text{O}_4$.

Crystallite size the particle size of the synthesized ferrite samples was estimated from x-ray broaden peak for the most intense peak (311) of diffraction peaks using Scherrer formula (1). The average crystallite size is (22 nm) for ferrite powders, while equal to 34 nm for ferrite samples sintered at (1373 K) as shown in Table (2). It is

observed that the average crystallite size increases with increase the amount of Mg^{2+} ions due to larger ionic radii than that of Ni^{2+} ions. Further, the average crystallite size of the samples increases with the increase sintering temperatures and this is due to the grain growth. Lattice constant was calculated using equation (2). Increasing the lattice constant caused by adding magnesium ions to Ni-Zn ferrite and Table (2) shows the lattice constant $a=0.835$ nm in the sample (E) and $a=0.838$ nm in the sample (G). Because larger Mg^{2+} (0.86\AA) ion radii as compared to the Ni^{2+} (0.80\AA) in octahedral site, replacement of smaller Ni^{2+} cations with larger Mg^{2+} cations causes an increase in lattice constant. The lattice constant of this ferrite was increased with increasing sintering temperature. X-ray density was calculated using relation (3); it relates with chemical composition of the sample and lattice parameter, it is observed that the x-ray density decreases with increasing magnesium ion content. This can be attributed to the substitution of heavier nickel ions by the lighter magnesium ions. Mg^{2+} ions have lower atomic weight than Ni^{2+} ion and this decrease in atomic weight causes a decrease in the X-ray density, another reason is increase in lattice constant when add Mg^{2+} ion. It is found that the x-ray density (theoretical density) decreases when a sample is sintered that is because of increase in the lattice constant.

Table (2) Lattice constant (\AA), Crystallite size (nm) and X-ray density (g/cm^3) of MgNiZn-ferrites.

ferrite	Temp. K	symbol	Lattice constant (\AA)	Crystallite size (nm)	x-ray density g/cm^3
E	773 K	$Ni_{0.6}Zn_{0.3}Mg_{0.1}Fe_2O_4$	0.835	22.02	5.06
G		$Ni_{0.4}Zn_{0.3}Mg_{0.3}Fe_2O_4$	0.838	22.68	4.86
E/1373	1373	$Ni_{0.6}Zn_{0.3}Mg_{0.1}Fe_2O_4$	0.8426	34.15	5.18
G/1373	K	$Ni_{0.4}Zn_{0.3}Mg_{0.3}Fe_2O_4$	0.848	52.15	5.01

Electrical properties of MgNiZn -ferrites

DC- Resistivity

Resistivity of the samples $Ni_{0.7-y}Zn_{0.3}Mg_yFe_2O_4$ ($y=0, 0.1, 0.2, 0.3$) calculated by the relation (4). It is found the resistivity decrease as a function of temperature shown in the Figure (7). The decrease in resistivity with increase in temperature is due to the increase in drift mobility of the charge carriers where present semi conducting behavior. However, when adding Mg ions in the Ni-Zn ferrites, the resistivity increase, as shown in Figure (6), due to Mg^{2+} ions are preferred B-site which avoid presence of divalent iron ion Fe^{2+} where obtain high resistivity. With increasing Mg^{2+} content only octahedral Fe^{2+} ions are substituted by Mg^{2+} so that the resistivity increase with increasing Mg^{2+} content.

Table (3) Resistivity (ohm.m) as a function of temp. of NiZnMg ferrite sintered at 1373⁰K.

Content of Mg ions (y)	Y= 0.0	Y= 0.1	Y= 0.2	Y= 0.3
ρ (ohm-m)at 300(k)	188733	544228	131878	444516
ρ (ohm-m)at 340(k)	107967	392129	73383	64166
ρ (ohm-m)at 380(k)	86792	21365	9431	102852
ρ (ohm-m)at 420(k)	25087	6602	3156	60130
ρ (ohm-m)at 460(k)	420	525	421	4257
ρ (ohm-m)at 500(k)	109	81	306	2940
ρ (ohm-m)at 540(⁰ k)	73	49	94	823

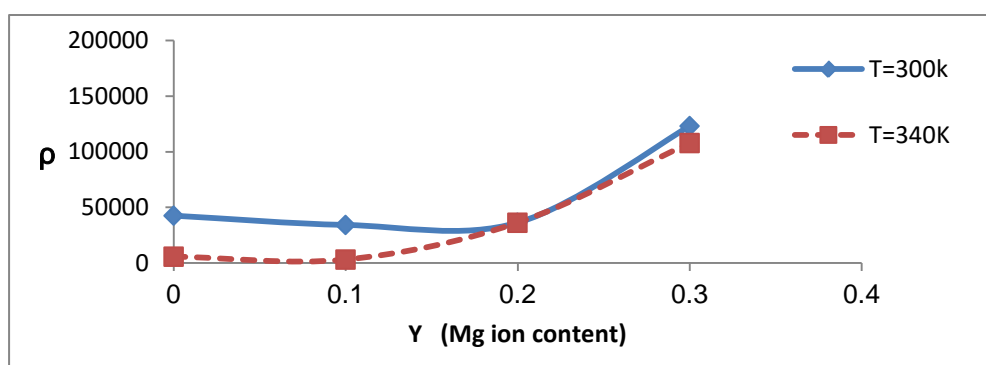


Figure (6) Represents the resistivity as a function of (y) Mg ion content in the NiZnMg ferrites.

Activation energy

The values of E_a are obtained from the slopes of the different straight lines curves in the Figure (7) .It is found that the activation energy increases when the add Mg^{+2} ions because of decrease in Fe^{+2} ions, reported above in the resistivity, as shown in Figure (8).

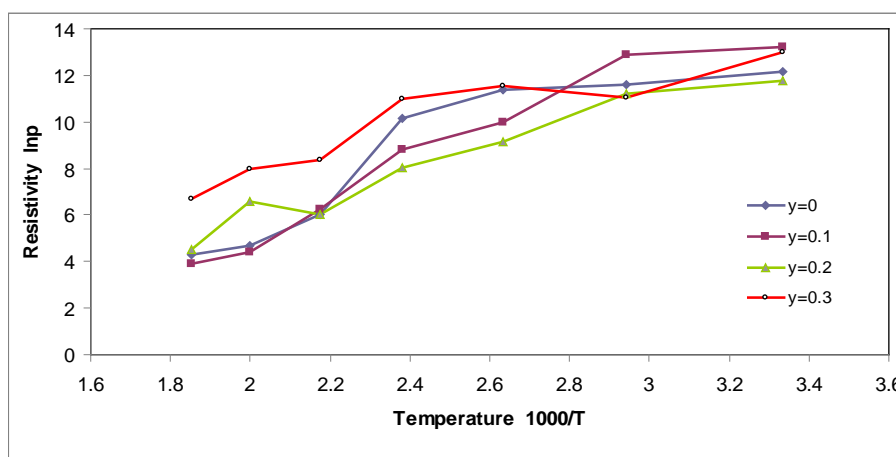


Figure (7) Represents resistivity as a function of temperature (1/T) of MgNiZn ferrites with different composition

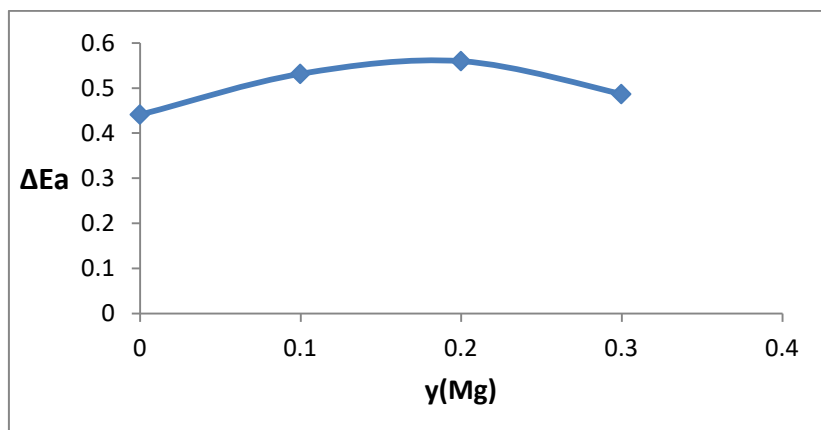


Figure (8) The activation energy as a function of Mg ion content in NiMgZn ferrite.

At high concentration of Mg^{2+} ions, where the conductivity is low due to the obstruction of Mg^{2+} ions to the hopping process between iron ions so the activation energy increase where the electron or holes need much energy to hopping from ion to another. Table (3) shows the activation energy of MgNiZn ferrites.

CONCLUSIONS

- 1- Nano crystalline NiZnMg-ferrite powders were successfully synthesized by the ignition of gel precursor upon heating at $200^{\circ}C$ (sol-gel auto combustion method).
2. For NiZnMg- ferrite composition, lattice constant, porosity and crystallite size increased but the x-ray density (theoretical density) decreased when the content of Mg ion is increased.
3. For NiZnMg-ferrite compositions, resistivity and activation energy increased when increasing of Mg ions.
4. In general it is shown that a smaller crystallite and grain sizes provides more barriers, as well as a larger boundary layer, which act to reduce the electron flow where the resistivity increases when the grain size decrease in Nano range. So that the value of resistivity at room temperature reaches more than 10^{+3} (ohm.m) with different compositions

REFERENCES

- [1]. Smit, J. H.P.J. Wijn, Ferrites, Jhon Wiley and Sons, New York, (1959)
- [2]. Goldman, "Recent Advances in Ferrite Materials Technology," in Modern Ferrite Technology, Van Nostr and Reinhold, New York, (1990)
- [3]. Nicola A. Spaldin, Magnetic Materials (Fundamentals and Applications), Second edition. University of California, Santa Barbara (2011)
- [4].MahRukh Siddiquah ,Department of Chemistry ,PhD thesis, Quaid-I-Azam University Islamabad, Pakstan, 2008 .
- [5]. David Sellmyer, Advanced Magnetic Nanostructures, Library of Congress Control Number: 2005935140, USA, (2006)

- [6]. Siti Soleha Jonit, Madzlan Aziz and Rita Sundari, Synthesis and Characteristic Study for the Magnesium Ferrite using Sol Gel Method , Empowering Science, Technology and Innovation Towards a Better Tomorrow, p.p.(340-345), Johor, Malaysia, (2011).
- [7]. Mukherjee, K. S.B. Majumder , Synthesis process induced improvement on the gas sensing characteristics of nano-crystalline magnesium zinc ferrite articles, *Sensors and Actuators B*, Vol. 162 pp.229– 236 , (2012)
- [8]. Srimala, A. A. S. and others, Low Temperature Synthesis of MgFe₂O₄ Soft Ferrite Nanocrystallites, *Journal of the Australian Ceramic Society* Vol. 46, No.1, pp.11-14, (2010).
- [9]. Cullity, B. D. 'Elements of X-Ray Diffraction', 2nd Ed, Addison-Wesley. INC. (1978).
- [10]. Griffiths, R. and C. Radford ; calculation ceramic . "maclaren and sons Ltd London, (1964).
- [11]. Singer, F. and S. S. Singer , "industrial ceramics ", chapman and hall Ltd London ,(1963).